JOURNAL OF AIRCRAFT
Vol. 33, No. 3, May–June 1996

Assessment of Noise Control Measures for a Model Advanced Ducted Propulsor

David G. Hall*
NYMA, Inc., Brook Park, Ohio 44142
and
Richard P. Woodward†
NASA Lewis Research Center, Cleveland, Ohio 44135

This article presents a study of estimated full-scale noise levels based on measured levels from the advanced ducted propulsor subscale model. Testing of this model was performed in the NASA Lewis Low Speed Anechoic Wind Tunnel at a simulated takeoff condition of Mach 0.2. Potential benefits of two noise control approaches were evaluated. The effect of active noise control (ANC) on the effective perceived noise level (EPNL) was evaluated by artificially removing various rotor/stator interaction tones. The effect of a passive exhaust duct liner on the fan EPNL was modeled by applying a predicted noise attenuation spectrum to the measured data. The effect of hybrid active–passive control (which implements both the ANC and passive exhaust duct liner), was also evaluated. EPNL values are approximate because the original source data were limited in bandwidth and in sideline angular coverage. The main emphasis is on comparisons between the baseline and configurations with simulated noise control measures.

Introduction

ACOUSTIC testing of the advanced ducted propulsor (ADP) model was conducted in the NASA Lewis Low Speed Anechoic Wind Tunnel. A previous report[1] was published documenting far-field results for sound pressure level (SPL). The present study uses these far-field SPL results as the raw data for calculating effective perceived noise level (EPNL) estimates from a large-scale ADP in the baseline configuration. The aircraft engine design community has shown considerable interest in applying active noise control (ANC) measures to turbofan engines.[2] This article explores the potential benefits of active noise control in a typical next-generation ducted fan by selectively removing the tone noise from the ADP data via digital filtering, and analyzing the improvement in estimated EPNL. In addition, passive noise control measures are simulated by applying various broadband attenuation curves to the control case data. Combined active–passive noise control measures are also evaluated.

Apparatus

Anechoic Wind Tunnel

The NASA Lewis 9- by 15-ft anechoic wind tunnel has a maximum airspeed in the test section of Mach 0.20, providing a takeoff/approach condition simulation. The tunnel acoustic treatment provides anechoic conditions down to a frequency of 250 Hz, which is lower than the frequency of any propeller acoustic tones expected from the ADP model.

Acoustic Instrumentation

The acoustic data used in the present study were acquired using a sideline traversing microphone probe, as shown in Fig. 1. This probe was equipped with two 0.64-cm (0.25-in.) condenser microphones. Data for this report were acquired using the outermost microphone, which was located 167 cm (66 in.) from the fan centerline. The probe could survey a sideline of approximately 20–140 deg relative to the plane of the fan. The probe was programmed to move with approximately constant angular velocity relative to the model. Each traverse took approximately 180 s to complete and provided 52 sideline acoustic measurements.

ADP Model

Detailed design parameters for the ADP model are documented in Ref. 1. The more relevant information is repeated here for convenience. The model was configured with 16 blades and either 22 or 40 stator vanes. The combination of 22 vanes and 16 blades generates rotor/stator interaction tones at the blade passing frequency (BPF), which propagate out of the duct.[3] The interaction tone at BPF, which is generated with the 40-vane stator, does not propagate (cutoff effect). The model was operated at the takeoff blade pitch angle of −11

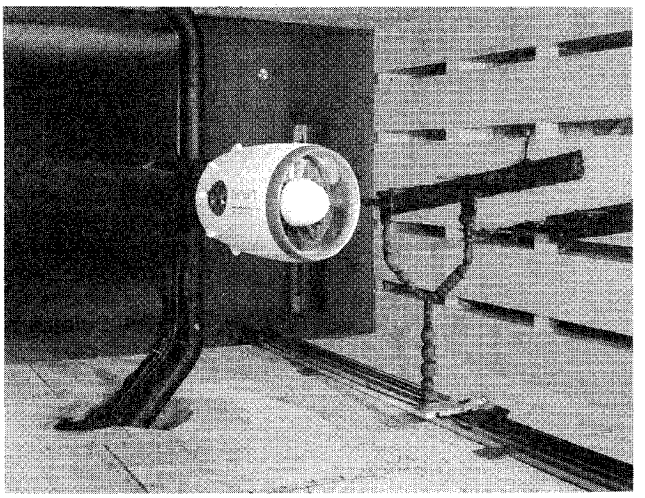

Fig. 1 ADP model installed in the 9- by 15-ft anechoic wind tunnel (shown with translating microphone probe).

Presented as Paper 93-4401 at the AIAA 15th Aeroacoustics Conference, Long Beach, CA, Oct. 25–27, 1993; received Oct. 22, 1994; revision received Dec. 22, 1995; accepted for publication Dec. 26, 1995.

*Senior Research Engineer, 2001 Aerospace Parkway. Member AIAA.

†Aerospace Engineer, M/S 77-6. Member AIAA.

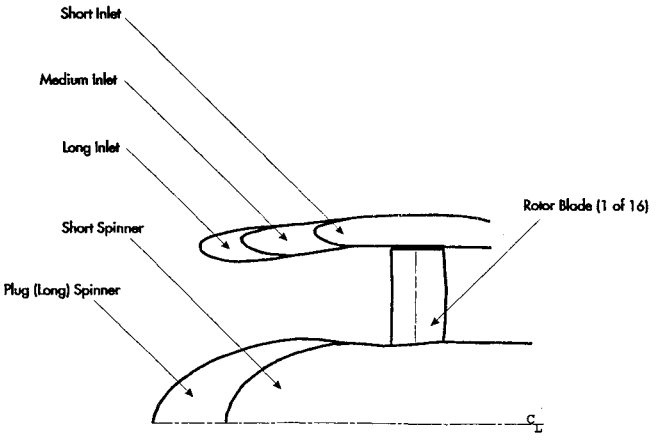

Fig. 2 Inlet and spinner configurations in the ADP model.

deg relative to cruise, with fan speeds of 84, 96, 102, and 107% relative to the design speed for the cases used in the present report. This provided subsonic tip speeds in all cases. Data were taken at windmill conditions as well, to provide an estimate of tunnel background level. A typical windmill SPL was at least 10 dB below the level observed with the fan running at its lowest speed (84% of design). The ADP installation provided a capability to rotate the model in the horizontal plane to provide a nonzero angle of attack relative to tunnel airflow. All of the data in this report were derived from cases with zero angle of attack. The model was driven by a compressed air turbine. There was no provision to simulate the noise effects of the core engine that would be present in a flight-configured engine. The model was configured with three different inlet geometries during this testing. The distance from the rotor stacking line to the inlet highlight was 12.09 cm (4.76 in.) for the short inlet, 21.03 cm (8.28 in.) for the medium inlet, and 26.14 cm (10.29 in.) for the long inlet.

A sketch of the inlet and spinner configuration is shown in Fig. 2. The majority of the data used in this report was collected with the short spinner configuration. Data for the case with 40-vane stator and short inlet include some cases with the plug or long spinner.

Data Analysis Procedure

During wind-tunnel testing, the traversing microphone signal was recorded using a digital spectrum analyzer. Each traverse produced 52 narrow-band spectra covering the range from 0 to 20 kHz with a resolution of 64 Hz. The upper bound of 20 kHz was chosen because it was the maximum capability of the available analyzer. In addition, this bandwidth permitted analysis of the first through sixth harmonic of the BPF tone for the ADP model. Each spectrum was the result of 12 frequency domain spectral averages. Some test conditions were recorded twice and analyzed for repeatability. Results indicated an uncertainty of approximately ± 1 dB. A probe position signal was also digitized and used to calculate the sideline angle for each of the 52 spectra. Typical sideline angular measurements were accurate to within 0.25 deg, including repeatability errors.

Postprocessing

A flow chart for the data processing operation used to produce results for this report is shown in Fig. 3. The following operations were performed:

1) Convert the spectrum analyzer data file from volts to units of pressure.

2) Perform a tunnel background correction by subtracting a spectrum taken under windmill conditions from the corresponding spectrum taken with the model under power.

3) Apply simulated noise control, if desired.

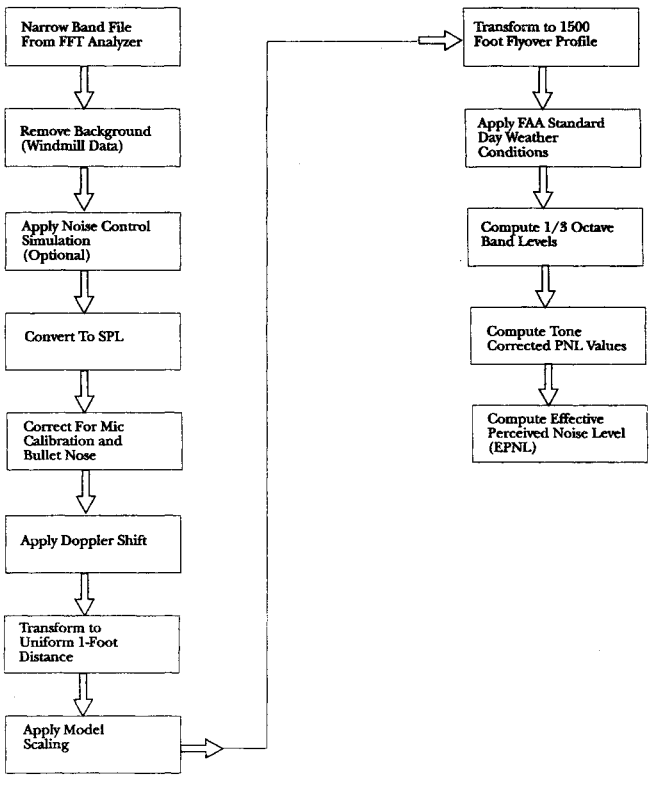

Fig. 3 Data processing flowchart.

4) Convert results to sound pressure level, in decibels relative to 20 μPa.

5) Correct for the microphone frequency response.

6) Correct for the frequency response of the bullet nose microphone windscreen.

7) Apply a Doppler shift to the spectral data, with the direction and magnitude of the shift calculated from sideline angle and tunnel airspeed.

8) Transform each spectrum to a standard radius of 1 ft, compensating for tunnel convection effects, spherical spreading, and atmospheric absorption.

9) Apply frequency and amplitude scaling to account for the model scale. The model fan diameter was 17.25 in. The projected full-scale fan radius is 118.25 in. The frequency shift scale factor is equal to 1:6.855. Amplitude scaling was done using the square of this value to account for the increase in thrust (proportional to inlet area).

10) Transform to a level flight path with flyover height of 1500 ft, accounting for spherical spreading and atmospheric absorption under FAA standard day conditions. This provided a single-engine simulation at a flight condition of Mach 0.2.

11) Synthesize one-third octave sound pressure levels from the narrow-band spectra.

12) Using the full set of 52 measurements, compute Noy-weighted one-third octave spectra, perceived noise level with tone correction (PNLT) vs time curves and EPNL estimates.

The simulated noise control option in step 3 was performed in a variety of ways. Active noise control was simulated by selectively removing the BPF tone or one of its harmonics down to the adjacent broadband level (see Fig. 4). When the tone removal was performed, it was done for all measured sideline angles. Broadband-only results were computed by removing the BPF tone and all of its harmonics. The effect of an exhaust duct liner was simulated by applying a broadband attenuation curve to all of the model-scale spectra with sideline angles greater than 100 deg. The maximum attenuation was 3 dB, at the center frequency. The frequency response of the liner model is shown in Fig. 5. This attenuation level is relatively low because the goal in this study was to model an

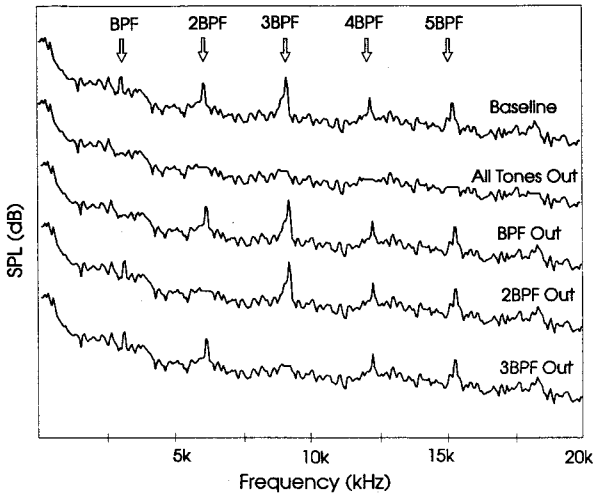

Fig. 4 Simulated ANC (waterfall plot).

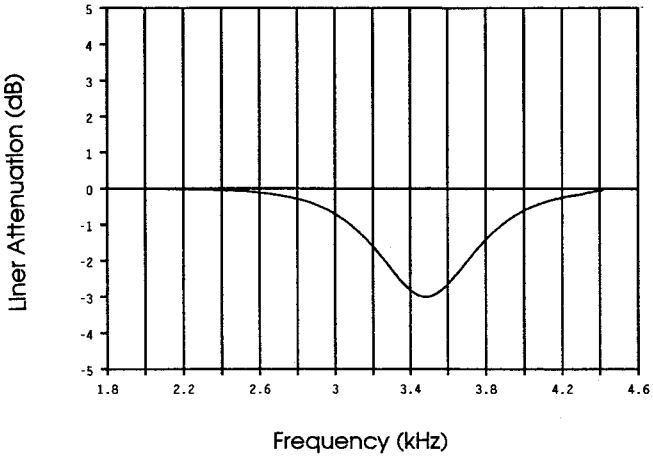

Fig. 5 Attenuation of typical simulated exhaust duct liner at model scale.

exhaust-duct-only liner with minimum system performance penalties such as added weight and increased drag. The use of an inlet duct liner was not modeled for similar reasons.

Three values of liner center frequency were evaluated: the first was designed for BPF at 100% speed (440 Hz at full scale, 3040 Hz at model scale); the second was designed for 2BPF (880 Hz at full scale, 6080 Hz at model scale); and the third liner was designed for a frequency that corresponded to the apparent peak in the broadband noise of the ADP (1470 Hz at full scale, 10 kHz at model scale). The methods of Ref. 4 were used to evaluate the approximate physical dimensions of these liners and ensure that they would be small enough to fit within the available space. The required length-to-height ratios *L/H* at full scale were estimated to be 0.67 (440-Hz liner), 1.0 (880-Hz liner), and 1.67 (1470-Hz liner). These values are consistent with the maximum space in the full-scale exhaust duct, which is expected to have a height of 32 in. and a length of 60 in. (*L/H* of 1.875). The maximum depth available for treatment was not considered.

EPNL Estimation

The computer program used to perform postprocessing step 12 was written to comply with the requirements of Ref. 5, including tone correction. The EPNL results are approximations because the bandwidth of the spectral data from the wind-tunnel tests was limited to 20 kHz. This translates to a full-scale frequency of 2918 Hz. Ignoring the effect of Doppler shift, the highest one-third octave frequency band that can be computed from this data is 2000 Hz. The FAA standard requires computation of one-third octave bands from 50 Hz to 10 kHz. Initially, it was thought that the sound energy in the model-scale data above 20 kHz might be significant. Two test cases were analyzed, using experimental data from 0 to 20 kHz plus broadband levels estimated via extrapolation in the range from 20 to 80 kHz. This provided narrow-band full-scale data adequate to allow synthesis of the one-third octave band levels up to and including the 10-kHz upper frequency limit. The first test case used the baseline data (no simulated noise control). The second test case had all of the BPF-related tones removed via digital filtering. The relative change in EPNL was approximately equal to the change observed when these two cases were run using the 0–20 kHz (model scale) spectra. From this, it was decided that the test data with limited frequency content (0–20 kHz) would be used for all subsequent analyses.

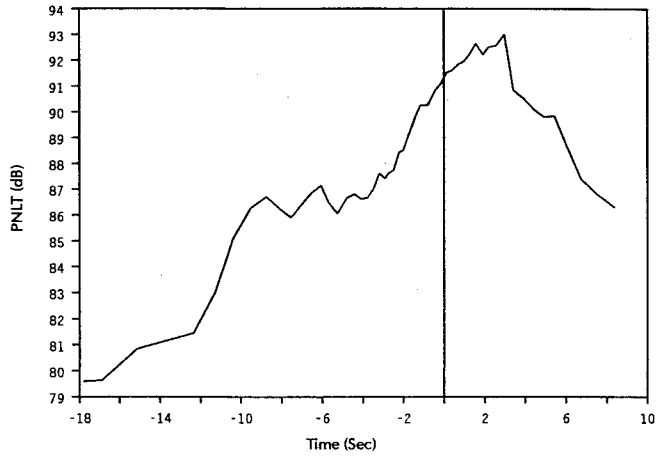

Fig. 6 Typical flyover noise profile; 40-vane model; 107% speed.

Additionally, the track traverse system was limited to sideline angles of approximately 20–140 deg. The FAA standard requires an SPL difference of 10 dB in PNLT between the peak value and the minimum at each end of the flyover. This was not feasible with the ADP data, since the traversing microphone probe did not move far enough to achieve a 10-dB dropoff at both ends in some cases. A typical plot of PNLT vs time is shown in Fig. 6.

Since the intention of this article is to assess the noise output of the baseline ADP model to its output with various noise reduction schemes in place, all of the EPNL estimates will be presented in decibels relative to a common, predefined reference level.

Analysis of Results

The results of this study are shown in Table 1. The column labeled Base in this table shows the relative EPNL estimate for the baseline model configuration. The column labeled BPF out shows the results when the BPF tone is removed (representing the effect of ANC) as shown in Fig. 4. The column labeled All tones out, shows the effect of removing the BPF tone and all of its harmonics. The intent is to show the relative importance of broadband noise to the EPNL values. The column labeled Liner @ BPF shows the effect of placing a simulated exhaust duct liner tuned to the frequency corresponding to BPF at 100% of the design speed. The column labeled Liner @ 2BPF shows the effect of a simulated exhaust duct liner tuned to 2BPF. The column labeled Liner @ 1470 shows the effect of an exhaust duct liner tuned to suppress broadband noise. The value of 1470 Hz is a full-scale frequency, and was chosen based on examination of a variety of the model-scale one-third octave spectra computed with all tones removed, which commonly peaked near 10 kHz (see Fig. 7a). 1470 Hz in full-scale corresponds to a frequency of 10 kHz in model-

Table 1 EPNL results in relative levels

Speed, %	Decibel, relative to baseline							
	Base	BPF out	All tones out	Liner at BPF	Liner at 2BPF	Liner at 1470	ANC + liner at 2BPF	ANC + liner at 1470
				40-vane stator, long inlet				
84	8.8	6.6	5.3	7.2	7.0	7.0	5.7	5.7
102	11.9	11.0	9.6	9.3	9.3	9.2	9.1	9.0
107	12.6	12.0	11.4	10.8	10.3	10.3	10.0	9.9
				40-vane stator, midlength inlet				
96	12.0	10.0	8.2	10.7	10.4	10.4	9.2	9.1
102	13.3	11.8	10.1	11.8	11.4	11.4	11.0	10.9
107	14.3	12.3	11.2	12.7	12.3	12.3	10.3	10.2
				40-vane stator, short inlet				
96	11.6	9.7	8.1	10.2	10.0	10.0	8.8	8.7
102	13.5	11.7	10.1	12.0	11.7	11.6	11.2	11.2
107	14.7	12.3	10.9	13.2	12.9	12.8	10.9	10.8
				22-vane stator, long inlet				
96	15.4	10.2	8.1	13.5	13.4	13.6	9.0	9.0
102	16.2	11.5	9.8	14.5	14.4	14.5	10.8	10.7
107	16.0	12.0	11.0	12.7	12.4	12.7	10.2	10.1
				22-vane stator, midlength inlet				
96	15.4	10.6	8.6	13.8	13.7	13.8	10.2	10.2
102	16.2	12.1	10.0	14.7	14.6	14.6	12.2	12.2
107	14.7	11.6	10.5	11.9	11.6	11.8	9.8	9.7
				22-vane stator, short inlet				
96	15.1	10.5	8.5	13.7	13.6	13.7	10.5	10.5
102	15.7	11.6	9.7	14.1	14.0	14.1	11.1	11.0
107	16.3	12.3	11.0	11.9	11.6	11.8	9.8	9.7
				22-vane stator, short inlet				
96	12.6	10.8	9.3	—	—	—	—	—
102	13.6	12.1	10.4	—	—	—	—	—
107	15.0	13.3	12.2	—	—	—	—	—

scale. A full-scale, NOY weighted spectrum, computed with all of the BPF-related tones removed, is shown in Fig. 7b.

The last two columns in Table 1 show the effect of hybrid active/passive noise control. The data in the column labeled ANC + liner @ 2BPF was computed by removing the BPF tone via digital filtering and applying the previously described liner model tuned to twice BPF. The column labeled ANC + liner @ 1470 shows the results when the BPF tone is suppressed using digital filtering and the liner is tuned to suppress broadband noise as described previously.

Some interesting observations may be made, based on the data in Table 1. It is important to consider one of the underlying assumptions in this study regarding the noise suppression models. The attenuation because of the simulated exhaust duct liner was applied only for sideline angles greater than 100 deg. Tone removal (simulating ANC) was applied for all sideline angles to simulate the effect of acoustic mode cancellation at the stator vanes, which could presumably give both inlet and exhaust duct tone suppression.

The effect of BPF tone removal on the 22-vane model is quite dramatic, with typical improvements in the 4–5 dB range. This is to be expected, since the BPF tone is cut-on in the 22-vane mode.

Table 1 shows that when the BPF tone is removed from the model configurations with the 40-vane stator and short spinner, EPNL reductions of 2 dB are typical. This number is rather large when one considers that the 40-vane model was designed to provide cutoff of the rotor/stator interaction tone at BPF. The reason for this reduction was the presence of residual BPF tone noise. Reference 6 provides a discussion of this residual noise, which was attributed to irregularities in the casing tip treatment. In the case of a device with a more fully suppressed BPF tone, it is likely that active noise control operating at BPF would provide very little EPNL reduction.

Results for the model configuration with the 40-vane stator, short inlet, and long spinner are also included in Table 1. EPNL reductions with BPF tone removal are similar to those observed with this inlet and the short spinner.

The effects of the three exhaust duct liner models are shown in Table 1 as well. EPNL was typically reduced by 2–3 dB, with the largest reductions occurring at the highest fan speeds. The center frequency of the liner model seems to have little effect on the noise suppression performance. If an exhaust duct liner is to be added to the production ADP, the choice of center frequency will likely be made based on mechanical considerations. The liner that is optimized for BPF suppression would require the smallest L/H ratio, but the greatest thickness. The liner that is optimized for broadband suppression would have the least thickness, but the largest L/H. If one assumes that the production engine has a stator vane count that provides cutoff of the BPF tone, and a modified casing tip treatment to remove the residual BPF noise, then the liner that is optimized for BPF suppression would probably not be chosen.

The relative merits of active control of the BPF tone vs the hybrid active/passive approach may be observed in Table 1. The data show the results when the BPF tone is removed via digital filtering and two alternate exhaust duct liners are applied. The first liner was tuned to 2BPF and the second was tuned for broadband suppression (1470 Hz at full scale). In

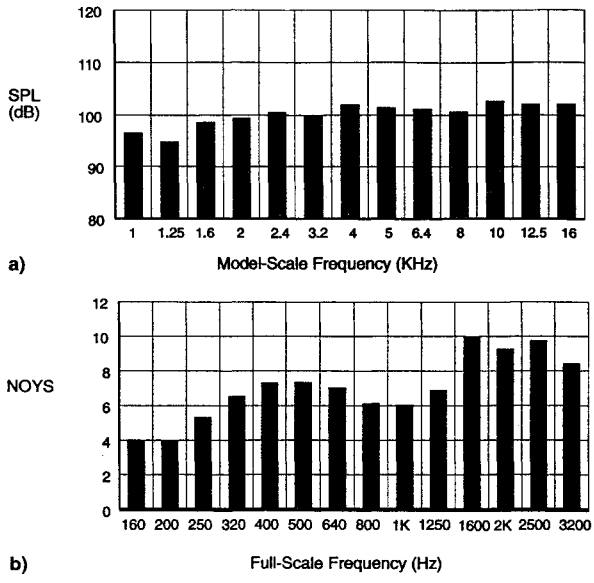

Fig. 7 Typical data with BPF-related tones removed, used to design broadband liner: a) one-third octave spectrum, as measured and b) Noy-weighted spectrum, full scale at flyover height (1500 ft).

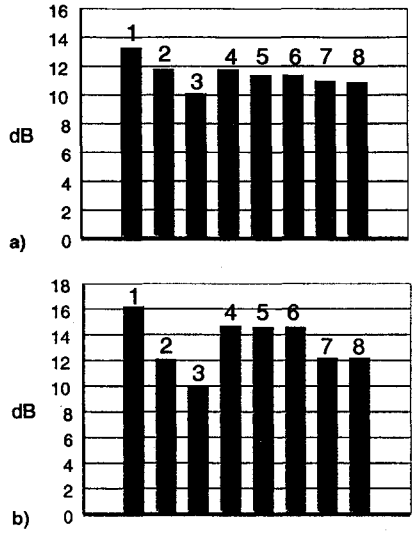

Fig. 8 Relative effect of all simulated noise control measures on EPNL (midlength inlet, 102% speed): a) 40- and b) 22-vane models. Key: 1, baseline (no noise control); 2, BPF removed; 3, all tones removed; 4, liner @ BPF; 5, liner @ 2*BPF; 6, liner tuned for broadband; 7, ANC + liner @ 2*BPF; and 8, ANC + broadband liner.

general, the use of the hybrid approach provides 1–2 dB of additional EPNL reduction over the active-only approach. The effect is most pronounced at the higher fan speeds. The improvement with hybrid noise control vs the baseline levels was approximately 3–4 dB with the 40-vane configurations and 5–6 dB with the 22-vane configurations. Thus, the hybrid active–passive approach offers only a modest improvement over the approach using active noise control alone for the ADP model. The relative effectiveness of any noise control measure will depend, in general, on the source noise characteristics.

A comparison of the relative merits of each of the simulated noise control approaches is shown in Fig. 8a for the 40-vane model, and in Fig. 8b for the 22-vane model. Data derived from Table 1 are plotted for the midlength inlet at 102% speed in each case. Note that, in the 40-vane case, the application of active noise control offers approximately the same benefit as the use of an exhaust duct liner. In the 22-vane case, suppression of the BPF tone is superior to the use of the exhaust duct liner. This is to be expected since ANC is applied at all sideline angles and the liner model only provided suppression for angles greater than 100 deg.

Broadband Results

Table 1 includes results that show the residual EPNL left when all of the BPF-related tones are removed. Typical results for the 40-vane cases show 3–4 dB of EPNL reduction. The improvement in the cases with 22-vane stators is approximately 5–6 dB. This indicates that some form of broadband noise suppression will be required before further gains can be made in noise reduction. The selection of a broadband noise reduction strategy must be made based on the identification of a dominant broadband noise source. Additional research is needed to evaluate the importance of the following sources: 1) interaction between turbulent rotor blade wakes and the stator vanes, 2) interaction between the rotating blades and the boundary layer on the spinner, 3) interaction between the rotating blades and the boundary layer on the duct wall, and 4) rotor-alone broadband noise.

Concluding Remarks

This report has presented EPNL estimates for the ADP model based on wind-tunnel data taken in the NASA Lewis Low Speed Anechoic Wind Tunnel. The experimental results were used to study the effect of adding simulated active/passive/hybrid noise control measures. In general, the suppression of the BPF tone yielded only modest noise reduction. This was partly because of the design of the ADP itself, since it included several features intended to suppress tone noise (low tip speed, large rotor/stator spacing, and cutoff BPF tone with the 40-vane stator). EPNL reduction for the 22-vane cut-on stator configuration was more significant. It is likely that current-generation turbofans, with more dominant tone noise, would benefit more from the application of active noise control than the ADP. Even so, the simulation results with the ADP model indicate a limit as to the maximum benefit available from tone noise reduction. Once the tones are gone, the broadband noise becomes the dominant source.

1) The reduction in estimated EPNL that was realized by fully suppressing the BPF tone via active noise control was approximately 2–3 dB with the cutoff stator and 4–5 dB with the cut-on stator.

2) Results obtained using a simulated passive exhaust duct liner showed that the EPNL reduction for the 40-vane model (BPF cutoff) was equivalent to the reduction obtained by suppressing the BPF via active noise control. With the 22-vane model (BPF cut-on), active noise control offered more improvement than the duct liner approach.

3) Hybrid noise control simulations (with the BPF tone removed via active noise control and an exhaust duct liner tuned for broadband suppression) yielded 1–2 dB of additional improvement in estimated EPNL over the case with BPF tone removal alone. Results for the cut-on and cutoff stator were equivalent.

4) EPNL estimates with all BPF-related tones removed indicate that broadband noise is a very important component in the overall acoustic output of this device. Future noise reduction efforts must take this fact into account. Additional research is needed to identify the dominant source of this broadband noise.

References

[1]Woodward, R. P., Bock, L. A., Heidelberg, L. J., and Hall, D. G., "Far-Field Noise and Internal Modes from a Ducted Propeller at Simulated Takeoff Conditions," NASA TM 105369, Jan. 1992; also

AIAA Paper 92-0371, Jan. 1992.
[2]Thomas, R., Burdesso, R., Fuller, C., and O'Brien, W., "Active Control of Fan Noise from a Turbofan Engine," AIAA Paper 93-0598, Jan. 1993.
[3]Tyler, J. M., and Sofrin, T. G., "Axial Flow Compressor Noise Studies," *SAE Transactions*, Vol. 70, 1962, pp. 309–332.
[4]Minner, G. L., and Rice, E. J., "Computer Method for Design of Acoustic Liners for Turbofan Engines," NASA TM X-3317, Oct. 1976.
[5]Federal Aviation Regulations, Vol. III, Pt. 36, Appendix A, Sec. 36.2.
[6]Heidelberg, L., and Hall, D., "Acoustic Mode Measurements in the Inlet of a Model Turbofan Using a Continuously Rotating Rake," AIAA Paper 93-0598, 1993.